

Sensitivity and entanglement in the avian chemical compass

Yiteng Zhang,¹ Gennady P. Berman,² and Sabre Kais^{3,4,*}

¹*Department of Physics, Purdue University, West Lafayette, Indiana 47907, USA*

²*Theoretical Division, LANL, and New Mexico Consortium, Los Alamos, New Mexico 87545, USA*

³*Department of Chemistry, Department of Physics, and Birck Nanotechnology Center, Purdue University, West Lafayette, Indiana 47907, USA*

⁴*Qatar Environment and Energy Research Institute, Qatar Foundation, Doha 5825, Qatar*

(Received 31 January 2014; revised manuscript received 28 May 2014; published 10 October 2014)

The radical pair mechanism can help to explain avian orientation and navigation. Some evidence indicates that the intensity of external magnetic fields plays an important role in avian navigation. In this paper, using a two-stage model, we demonstrate that birds could reasonably detect the directions of geomagnetic fields and gradients of these fields using a yield-based chemical compass that is sensitive enough for navigation. Also, we find that the lifetime of entanglement in this proposed compass is angle dependent and long enough to allow adequate electron transfer between molecules.

DOI: [10.1103/PhysRevE.90.042707](https://doi.org/10.1103/PhysRevE.90.042707)

PACS number(s): 87.10.-e, 03.65.Ud

I. INTRODUCTION

The navigational ability of birds has been a subject of interest for centuries. Every year migrant birds fly hundreds to thousands of miles between their seasonal habitats. Researchers have been trying to explain this astonishing phenomenon for decades. The radical pair mechanism (RPM) is a promising hypothesis to explain this extraordinary phenomenon [1–8]. This RPM was first proposed by Schulten *et al.* based on the fact that low magnetic fields can alter the rates and the yields of photochemical reactions [1]. This mechanism has been supported by a series of behavioral experiments [9–13] which indicate that the avian compass depends on both inclination and light intensity. Also, the photoreceptor cryptochrome located in the avian retina is involved in this hypothesis [14–22].

Both theoretical and experimental studies have revealed that the internal anisotropic hyperfine interaction is the key factor for a radical-pair-based compass to detect the presence of an external magnetic field and its direction [1,23–28]. The hyperfine interaction has been modeled and simulated in order to understand how to optimize the sensitivity of the chemical compass [29]. Also, the role of quantum coherence and entanglement in the chemical compass has been discussed [6,30–34]. In addition, some research has been done using this theory to design devices to detect the external weak magnetic fields [26,35–37].

There are still many aspects of this theory that remain to be studied to improve this mechanism. For instance, the fact that birds can use not only the inclination but also the intensity of geomagnetic fields for navigation has been demonstrated by early behavioral experiments [38,39]. Also, by comparing the long-distance migration routes and maps of geomagnetic field total intensity [40,41], one can observe that the migration routes are mostly along the direction of gradient of the magnetic field intensities. However, little theoretical or computational research has been done to explore this feature of bird navigation.

In this paper, we study the magnetic field sensitivity of a yield-based chemical compass in birds to explore how the

intensity of geomagnetic fields could be utilized in a yield-based compass. We also explore the angle dependence of the magnetic field effect on the yields of radical pairs. In addition, we examine entanglements in the reaction process of the RPM to explore the role that entanglement plays in this mechanism.

II. MODEL

There are many articles that model the avian compass, but only a few of them examine a two-stage scheme. Here we consider a two-stage scheme for the radical pair mechanism based on the proposed reactions that occur in the photoreceptor molecule, cryptochrome [42]. The initial radical pair [FAD•⁻ TrpH•⁺] is formed by light-induced electron transfer, followed by protonation and deprotonation, forming a secondary radical pair [FADH• Trp•]. This two-stage scheme is shown in Fig. 1. Both radical pairs are affected not only by the external magnetic field but also by their surrounding nuclei. Respectively, the Hamiltonians of the initial and secondary radical pair are

$$H_1 = g\mu_B \sum_{i=1}^2 \vec{S}_i \cdot (\vec{B} + \hat{A}_{1i} \cdot \vec{I}_i), \quad (1)$$

$$H_2 = g\mu_B \sum_{i=1}^2 \vec{S}_i \cdot (\vec{B} + \hat{A}_{2i} \cdot \vec{I}_i). \quad (2)$$

In Eqs. (1) and (2), \vec{S}_i is the unpaired electron spin of the radical pairs and \vec{I}_i is the nuclear spin of nitrogen in the pairs. We calculate the hyperfine coupling tensors (Table I) \hat{A}_{ij} using GAUSSIAN09 with UB3LYP/EPR-II. For simplicity, we only use one of the hyperfine coupling tensors within each molecule for our subsequent calculations, since additional nuclear spins have little effect on the yield curves [31]. Also, because the electron is located near the nitrogen atoms and the couplings between the electron and the nitrogen atoms are stronger than the couplings to other nearby hydrogen atoms, we choose the hyperfine coupling tensors associated with the nitrogen atoms in each molecule for our subsequent calculations. \vec{B} is the weak external geomagnetic field and depends on the angles θ and φ with respect to the reference frame of the immobilized radical pair (Fig. 2), i.e., $\vec{B} = B_0(\sin \theta \cos \varphi, \sin \theta \sin \varphi, \cos \theta)$. We

*kais@purdue.edu

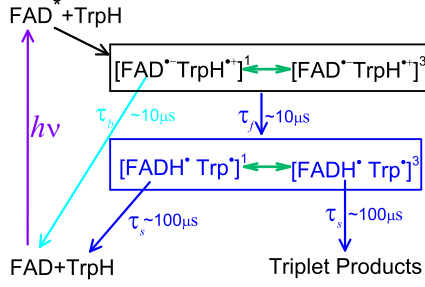


FIG. 1. (Color online) The reaction scheme of the radical pair mechanism in cryptochrome. $k_b = \tau_b$ and $k_f = \tau_f$ are the first-order rate constants for recombination of the initial radical pair and formation of the secondary pair from the initial one, respectively. $k_s = \tau_s$ is the rate constant for the decay of the secondary pair. The green two-headed arrows indicate the interconversion of the singlet and triplet states of the radical pairs.

can choose the x axis so that the azimuthal angle φ is 0. The constants g and μ_B are the g factor and the Bohr magneton of the electron, respectively.

The dynamics of the radical pairs in the two-stage scheme is governed by the following coupled Liouville equations [7,23,30,43–45]:

$$\begin{aligned} \dot{\rho}_1(t) = & -\frac{i}{\hbar}[H_1, \rho_1(t)] - \frac{k_f}{2}\{Q^S, \rho_1(t)\} \\ & - \frac{k_f}{2}\{Q^T, \rho_1(t)\} - \frac{k_b}{2}\{Q^S, \rho_1(t)\}, \end{aligned} \quad (3)$$

$$\begin{aligned} \dot{\rho}_2(t) = & -\frac{i}{\hbar}[H_2, \rho_2(t)] + \frac{k_f}{2}\{Q^S, \rho_1(t)\} + \frac{k_f}{2}\{Q^T, \rho_1(t)\} \\ & - \frac{k_s}{2}\{Q^S, \rho_2(t)\} - \frac{k_s}{2}\{Q^T, \rho_2(t)\}, \end{aligned} \quad (4)$$

TABLE I. HFC tensors of some atoms.

Molecule	Atom	Isotropy (G)	Anisotropy (G)	Principle axis (Å)
TrpH \bullet^+	N	12.864	-7.154	0.63 0.70-0.34
			-7.051	0.73 0.63 0.04
			14.205	-0.26 0.22 0.94
	H	-3.054	-1.478	0.50 0.86-0.12
			-0.977	-0.14 0.20 0.96
			2.454	0.85-0.47 0.22
FAD \bullet^-	N	2.339	-5.392	0.61 0.79 0.00
			-5.353	0.79 0.61 0.00
			10.745	0.00 0.00 1.00
			19.247	0.15 -0.07 0.99
Trp \bullet	N	8.393	-9.708	-0.23 0.97 0.10
			-9.539	0.96 0.24 -0.14
			19.247	0.15 -0.07 0.99
			-0.792	0.21-0.06 0.98
			1.320	0.75-0.63-0.20
FADH \bullet	N	2.015	-4.815	0.79 0.61 0.00
			-4.702	0.61 0.79 0.00
			9.517	0.00 0.00 1.00
	H	-3.054	-1.478	-0.50 0.86-0.12
			-0.977	-0.14 0.20 0.96
			2.454	0.85-0.47 0.22

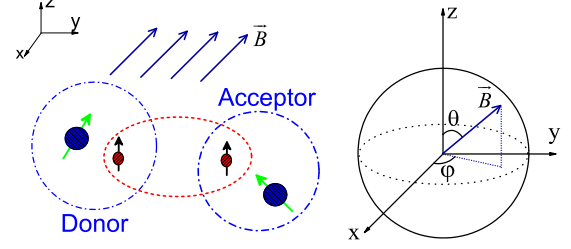


FIG. 2. (Color online) Left: A coupled radical pair with neighboring effective nuclear spins (green arrows, \rightarrow) in an external magnetic field \vec{B} (blue arrows, \rightarrow). Right: The direction of \vec{B} depicted in the molecular coordinate frame, where the z axis is the z axis of the radical pair [23].

where H_1 and H_2 are the Hamiltonians of the two radical pairs given in Eqs. (1) and (2); ρ_1 is the density matrix of the initial radical pair and ρ_2 is that of the secondary radical pair, which can be created from ρ_1 ; Q^S is the singlet projection operator, $Q^S = |S\rangle\langle S|$, and $Q^T = |T_+\rangle\langle T_+| + |T_0\rangle\langle T_0| + |T_-\rangle\langle T_-|$ is the triplet projection operator, where $|S\rangle$ is the singlet state and $(|T_+\rangle, |T_0\rangle, |T_-\rangle)$ are the triplet states; and all of the decay rates are indicated in Fig. 1. In addition, the initial state of the pair $[\text{FAD}\bullet^-\text{TrpH}\bullet^+]$ is assumed to be in the singlet state, $|S\rangle = \frac{1}{\sqrt{2}}(|\uparrow\downarrow\rangle - |\downarrow\uparrow\rangle)$, while the pair $[\text{FADH}\bullet\text{Trp}\bullet]$ is not produced initially. In other words, $\rho_1(0) = \frac{1}{9}\hat{I}_N \otimes Q^S$, where the electron spins are in the singlet states, and nuclear spins are in thermal equilibrium, a completely mixed state, which is a 9×9 identity matrix, and $\rho_2(0) = 0$.

This model would appear somewhat unrealistic since we neglect the environmental noise. However, our intention here is not to interpret experimental data accurately, which has been done in Ref. [42], but rather to explore limiting cases to discover to what extent the triplet yields are sensitive to the intensities of the external magnetic field. There are many papers that discuss the effects of noise on the radical pair mechanism [29,31]. Intuitively, one might expect that dephasing noise is unfavorable for the function of the chemical compass. However, these studies show that the effect of noise depends on the model. In the model of Gauger *et al.*, the compass mechanism is almost immune to pure phase noise [31]. Cai *et al.* argued that correlated dephasing noise could even enhance the chemical compass in their model [29]. Both models give us positive, or at least non-negative, perspectives concerning dephasing noise. Therefore we neglect dephasing noise in this paper.

Also, we consider the product formed by the radical pair $[\text{FADH}\bullet\text{Trp}\bullet]$ in the triplet state as the signal product, whose yield is defined as $\Phi_T = k_s \int_0^\infty \text{Tr}[Q^T \rho(t)] dt$ [7,46,47], where $Q^T = |T\rangle\langle T|$, and $|T\rangle = |T_+\rangle + |T_0\rangle + |T_-\rangle$.

III. RESULTS AND DISCUSSION

First, we look at the magnetic field effect (MFE) on the signal yields. We consider $\Delta\Phi_T/\Phi_{0T}$ as a metric of the magnetic field effect, where Φ_{0T} is the signal yield at zero field and $\Delta\Phi_T$ is the difference between the signal yields at a given field (Φ_T) and Φ_{0T} . In Fig. 3, we can clearly see that the angle

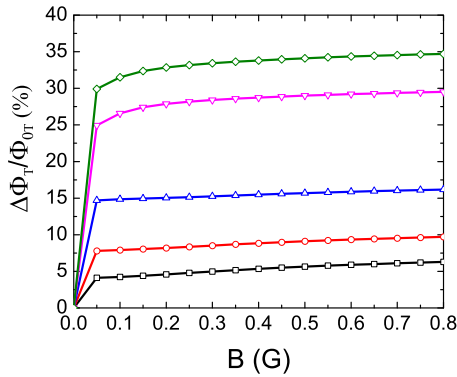


FIG. 3. (Color online) Angle dependence of the magnetic field effect as a function of the external field. The MFE is the ratio of the difference between the triplet yields of the secondary pair at nonzero external fields and zero field ($\Delta\Phi_T = \Phi_T - \Phi_{0T}$) and the triplet yields at zero field, which is $\Delta\Phi_T/\Phi_{0T}$. This graph depicts the MFE as a function of external fields \vec{B} for five different polar angles θ between the electron spin and the magnetic field. $\theta = 0^\circ$ (black, $-\square-$), 30° (red, $-o-$), 60° (blue, $-\triangle-$), 85° (pink, $-\nabla-$), and 90° (green, $-\diamond-$). The decay rates are shown in Fig. 1.

plays a very important role in the MFE. As the angle increases, the MFE becomes more and more significant. The yields are barely changed, around 5%, when the angle is 0° . However, the MFEs are very significant at 85° and 90° , since the yield changes are greater than 25%. The MFE is even greater than 30% at 90° . Such a significant effect, possibly exceeding the environmental noise, could induce a physiological reaction in birds, making this yield-based chemical compass feasible for birds. In other words, since the geomagnetic field has a significant effect on the yields of radical pair reactions along the parallels, which are distinguished by latitudes, it is easier for birds to detect the direction of parallels. As we know, the climate can mainly be affected by the parallels and the birds immigrate according to the climate. Therefore this feature may be a result of the natural selection.

Having estimated the role of MFE on the signal yields, we now focus on the magnetic sensitivity of the avian compass, which is defined as $\partial\Phi_T/\partial B$ (T^{-1}) [34,48]. From the dependence of the MFEs on polar angles (Fig. 3), we speculate that birds can detect the direction of parallels. The magnetic sensitivity at a magnetic field of 0.5 G for various angles (Fig. 4) also confirms this conjecture. Figure 4 shows that the sensitivities around 0° and 90° are similar and also larger than for most other angles, which could indicate that the birds can detect the directions of meridians and parallels if they use the intensity of the magnetic field for navigation, since the yield-based compass is most sensitive along these two directions. Another property that attracted our attention is that the sensitivity's slope is significantly larger between 80° and 90° than that of the other sections of the curve. Along with the MFEs, this property of rapidly increasing sensitivity may imply that it is easier for birds to detect the direction of parallels than that of meridians. Since the yield-based compass is very sensitive to the change of intensities, we can also expect that it is easier for birds to detect the change of the field intensities

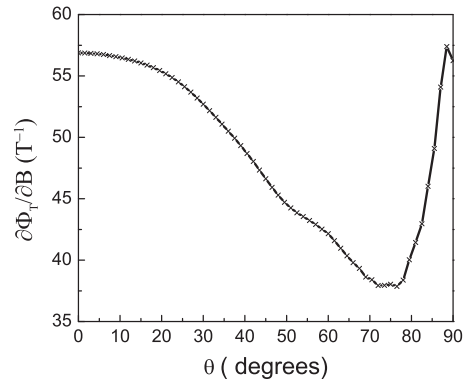


FIG. 4. The magnetic sensitivity of the chemical compass as a function of angle. The sensitivity is defined as $\partial\Phi_T/\partial B$ in T^{-1} . There is a rapid increase in this sensitivity between 80° and 90° . The sensitivity under geomagnetic field is of the order of 10^{-3} , requiring a strong magnification mechanism in birds to utilize it.

when the polar angle is around 90° . This capability can enable the birds to migrate along the direction of the gradient of intensities of the geomagnetic fields.

Furthermore, we explore the magnetic sensitivity as a function of the intensities of the magnetic field for several polar angles θ in Fig. 5. Figure 5 shows two types of curves. The first pattern is observed for 85° and 90° in which the sensitivities monotonically decrease as the external fields increase. In this situation, the sensitivities are much higher for very weak magnetic fields, less than 0.25 G, than those in the normal range of the geomagnetic fields, from 0.25 to 0.65 G [41]. The sensitivities fall into the normal range in the geomagnetic fields, similar to other angles. The other pattern occurs for 0° , 30° , and 60° , and the sensitivities increase initially and then decrease as the external fields increase. In this situation, the maxima of the curves move rightwards and downwards as the polar angles increase. Combining these two situations (Fig. 5), we observe the properties of the chemical compass

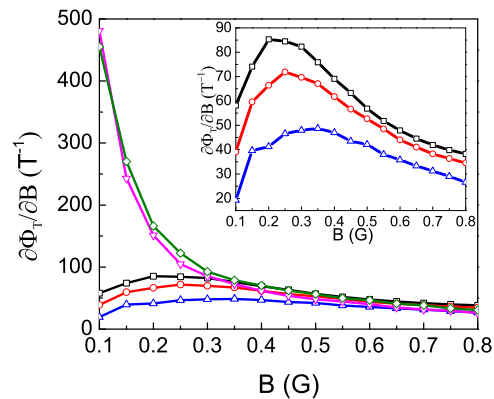


FIG. 5. (Color online) Intensity dependence of the magnetic sensitivity. This graph shows the sensitivity as a function of external magnetic field \vec{B} as a function of polar angle θ between the z axis of the radical pair and the magnetic field, i.e., $\theta = 0^\circ$ (black, $-\square-$), 30° (red, $-o-$), 60° (blue, $-\triangle-$), 85° (pink, $-\nabla-$), and 90° (green, $-\diamond-$). The interior graph magnifies the data for angles $\theta = 0^\circ$ (black, $-\square-$), 30° (red, $-o-$), and 60° (blue, $-\triangle-$).

mentioned before, namely, that compass is most magnetically sensitive around 0° and 90° at geomagnetic fields. However, above 0.35 G, all sensitivities decrease as the fields' intensities increase. This may explain why some species of birds lose their ability to orient themselves in higher magnetic field [9,23]. Also, since the sensitivity is not zero, after exposure to unnatural magnetic fields for a long time the birds may adapt to the decreased sensitivity so that they are able to regain the ability to orient [49].

In Figs. 4 and 5, the change of yields is very small, of the order of 10^{-3} , under the geomagnetic field. However, it has been suggested but not verified that birds may be able to amplify such weak signals to a biologically useful level [23]. If we choose a suitable amplification factor based on the hypothesis that birds can also use their vision for navigation, birds can exploit the weak signal [23]. Also, different theoretical models may result in different yield contrasts. Therefore the need for amplification is not as strong in some models as in others.

Entanglement is believed to play an important role in many systems [50–53], including the chemical compass in birds. In this paper, we use negativity as the metric of entanglement, $N(\rho) = \frac{\|\rho^{TA}\|_1 - 1}{2}$, where $\|\rho^{TA}\|_1$ is the trace norm of the partial transpose of the system's density matrix [50,54]. However, for the two-stage scheme, the secondary radical pair barely has any entanglement between the two unpaired electrons, since the chemical reaction has destroyed the entanglement between them in the preceding radical pair [FAD \bullet^- TrpH \bullet^+]. The unpaired electrons in the initial radical pair show a robust entanglement. Figure 6 shows the entanglement of the initial radical pair [FAD \bullet^- TrpH \bullet^+] for four polar angles, θ . Also, the dynamics of the entanglement is clearly dependent on the

angles, which is very different from the results in the one-stage case [33]. However, the entanglements at 0° , 30° , and 60° are nearly the same for the first $0.1\mu s$, while the entanglement at 90° is very different from the others. At 90° , the entanglement lasts for $0.1\mu s$, which is long enough for electrons to transfer between different molecules [55].

IV. CONCLUSIONS

We have studied the role of the intensity of the magnetic field in avian navigation. It appears that birds need a strong amplification mechanism to magnify the weak signals, although this mechanism is still unknown. The properties around 90° , i.e., the direction of parallels, stand out from those at other angles for magnetic sensitivity and entanglement. When the birds migrate thousands of miles, they might be able to detect the change of the intensity of geomagnetic fields and the approximate direction of parallels instead of sensing the exact direction. Our simulations provide some preliminary justification. We also examined different hyperfine tensors to calculate the angle dependence of sensitivity for a field of 0.5 G (Fig. 7). The result also shows that the magnetic sensitivity is extraordinarily high around 90° , although the sensitivity at 0° becomes very low, giving support to our conjecture that the birds are able to detect the approximate direction of parallels.

This research also demonstrated that birds can use head scans to determine orientation [56]. By using head scans, they may adjust the polar angle (Fig. 2) to try to find the direction of parallels. After finding the direction of parallels, they can make the chemical compass most sensitive to the change of intensities of geomagnetic fields along such a direction, so that they can fly along the direction of the gradient of the intensities. Therefore, by detecting the directions of parallels and the gradient of the intensities of geomagnetic fields, the birds are able to migrate thousands of miles.

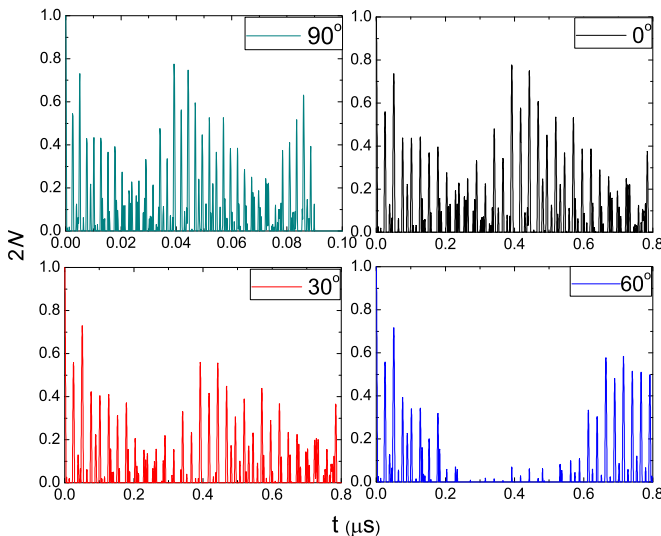


FIG. 6. (Color online) Entanglement of the initial radical pair [FAD \bullet^- TrpH \bullet^+] as a function of external fields for four polar angles, $\theta = 0^\circ$ (black), 30° (red), 60° (blue), and 90° (green). Since the entanglement of the initial pair [FAD \bullet^- TrpH \bullet^+] is compressed within $0.1\mu s$, the time scale of the graph for that is from 0 to $0.1\mu s$. The other graphs range from 0 to $0.8\mu s$, and the entanglement of the initial pair at 0° , 30° , and 60° differ after $0.3\mu s$.

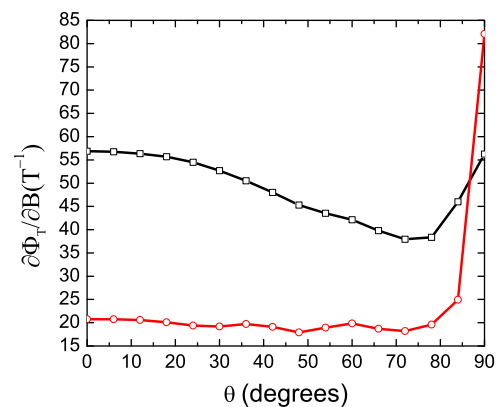


FIG. 7. (Color online) The magnetic sensitivity as a function of angles under different hyperfine coupling tensors. The black curve ($-\square-$) describes the situation under the hyperfine tensor mentioned in the previous context, while the red one ($-\circ-$) shows the situation under a different set of hyperfine tensors, $diag\{\hat{A}_{11}\} = \{-0.650\text{ G}, -0.566\text{ G}, 17.071\text{ G}\}$, $diag\{\hat{A}_{12}\} = \{5.71\text{ G}, 5.81\text{ G}, 27.07\text{ G}\}$, $diag\{\hat{A}_{21}\} = \{-0.792\text{ G}, -0.692\text{ G}, 14.060\text{ G}\}$, $diag\{\hat{A}_{22}\} = \{-1.32\text{ G}, -1.15\text{ G}, 27.64\text{ G}\}$.

In our study, we neglect environmental noise. However, the molecular environment is an important factor affecting the hyperfine coupling tensor. Although it is beyond the scope of this paper, the aqueous environment is essential for the interaction between cryptochrome and $\text{TrpH}\bullet^+$, since water molecules have an important role in the hyperfine coupling constants in $\text{TrpH}\bullet^+$ [57].

ACKNOWLEDGMENTS

We would like to thank the NSF Center for Quantum Information for Quantum Chemistry (QIQC), Award No. CHE-1037992, for financial support. We are also thankful to Gary Doolen for useful comments.

-
- [1] K. Schulten, C. E. Swenberg, and A. Weller, *Z. Phys. Chem.* **111**, 1 (1978).
- [2] T. Ritz, R. Wiltschko, P. J. Hore, C. T. Rodgers, K. Stapput, P. Thalau, C. R. Timmel, and W. Wiltschko, *Biophys. J.* **96**, 3451 (2009).
- [3] J. C. S. Lau, N. Wagner-Rundell, C. T. Rodgers, N. J. B. Green, and P. J. Hore, *J. R. Soc., Interface* **7**, S257 (2010).
- [4] J. C. S. Lau, C. T. Rodgers, and P. J. Hore, *J. R. Soc., Interface* **9**, 3329 (2012).
- [5] S. F. Huelga and M. B. Plenio, *Contemp. Phys.* **54**, 181 (2013).
- [6] I. K. Kominis, *Chem. Phys. Lett.* **542**, 143 (2012).
- [7] A. T. Dellis and I. K. Kominis, *Biosystems* **107**, 153 (2012).
- [8] I. K. Kominis, *Phys. Rev. E* **83**, 056118 (2011).
- [9] W. Wiltschko and R. Wiltschko, *Science* **176**, 62 (1972).
- [10] W. Wiltschko, U. Munro, H. Ford, and R. Wiltschko, *Nature (London)* **364**, 525 (1993).
- [11] W. Wiltschko and R. Wiltschko, *J. Comp. Physiol. A* **177**, 363 (1995).
- [12] W. Wiltschko and R. Wiltschko, *Naturwissenschaften* **85**, 164 (1998).
- [13] W. Wiltschko and R. Wiltschko, *J. Comp. Physiol. A* **184**, 295 (1999).
- [14] H. Mouritsen, U. Janssen-Bienhold, M. Liedvogel, G. Feenders, J. Stalleicken, P. Dirks, and R. Weiler, *Proc. Natl. Acad. Sci. USA* **101**, 14294 (2004).
- [15] M. Liedvogel, K. Maeda, K. Henbest, E. Schleicher, T. Simon, C. R. Timmel, P. J. Hore, and H. Mouritsen, *PLoS ONE* **2**, e1106 (2007).
- [16] K. B. Henbest, K. Maeda, P. J. Hore, M. Joshi, A. Bacher, R. Bittl, S. Weber, C. R. Timmel, and E. Schleicher, *Proc. Natl. Acad. Sci. USA* **105**, 14395 (2008).
- [17] O. Efimova and P. J. Hore, *Biophys. J.* **94**, 1565 (2008).
- [18] S.-R. Harris, K. B. Henbest, K. Maeda, J. R. Pannell, C. R. Timmel, P. J. Hore, and H. Okamoto, *J. R. Soc., Interface* **6**, 1193 (2009).
- [19] T. Ritz, T. Yoshii, C. Helfrich-Foerster, and M. Ahmad, *Commun. Integr. Biol.* **3**, 24 (2010).
- [20] H. Mouritsen and P. J. Hore, *Curr. Opin. Neurobiol.* **22**, 343 (2012).
- [21] C. Nießner, S. Denzau, K. Stapput, M. Ahmad, L. Peichl, W. Wiltschko, and R. Wiltschko, *J. R. Soc., Interface* **10**, 20130638 (2013).
- [22] C. A. Dodson, P. J. Hore, and M. I. Wallace, *Trends Biochem. Sci.* **38**, 435 (2013).
- [23] T. Ritz, S. Adem, and K. Schulten, *Biophys. J.* **78**, 707 (2000).
- [24] C. R. Timmel, F. Cintolesi, B. Brocklehurst, and P. J. Hore, *Chem. Phys. Lett.* **334**, 387 (2001).
- [25] F. Cintolesi, T. Ritz, C. W. M. Kay, C. R. Timmel, and P. J. Hore, *Chem. Phys.* **294**, 385 (2003).
- [26] K. Maeda, K. B. Henbest, F. Cintolesi, I. Kuprov, C. T. Rodgers, P. A. Liddell, D. Gust, C. R. Timmel, and P. J. Hore, *Nature (London)* **453**, 387 (2008).
- [27] C. T. Rodgers and P. J. Hore, *Proc. Natl. Acad. Sci. USA* **106**, 353 (2009).
- [28] K. Maeda, C. J. Wedge, J. G. Storey, K. B. Henbest, P. A. Liddell, G. Kodis, D. Gust, P. J. Hore, and C. R. Timmel, *Chem. Commun.* **47**, 6563 (2011).
- [29] J. Cai, F. Caruso, and M. B. Plenio, *Phys. Rev. A* **85**, 040304 (2012).
- [30] I. K. Kominis, *Phys. Rev. E* **86**, 026111 (2012).
- [31] E. M. Gauger, E. Rieper, J. J. L. Morton, S. C. Benjamin, and V. Vedral, *Phys. Rev. Lett.* **106**, 040503 (2011).
- [32] H. J. Hogben, T. Biskup, and P. J. Hore, *Phys. Rev. Lett.* **109**, 220501 (2012).
- [33] J. A. Pauls, Y. Zhang, G. P. Berman, and S. Kais, *Phys. Rev. E* **87**, 062704 (2013).
- [34] J. Cai, G. G. Guerreschi, and H. J. Briegel, *Phys. Rev. Lett.* **104**, 220502 (2010).
- [35] G. Kodis, P. A. Moore, T. A. Moore, and D. Gust, *J. Phys. Org. Chem.* **17**, 724 (2004).
- [36] J. Cai, *Phys. Rev. Lett.* **106**, 100501 (2011).
- [37] J. Cai and M. B. Plenio, *Phys. Rev. Lett.* **111**, 230503 (2013).
- [38] J. H. Fisher, U. Munro, and J. B. Phillips, *Avian Migration*, edited by P. Berthold (Springer, Berlin, 2003), pp. 423–432.
- [39] W. Wiltschko and R. Wiltschko, *J. Comp. Physiol. A* **191**, 675 (2005).
- [40] I. Newton, *The Migration Ecology of Birds* (Academic Press, New York, 2008).
- [41] S. Maus, S. Macmillan, S. McLean, B. Hamilton, A. Thomson, M. Nair, and C. Rollins, The US/UK World Magnetic Model for 2010-2015, NOAA Technical Report NESDIS/NGDC (2010).
- [42] K. Maeda, A. J. Robinson, K. B. Henbest, H. J. Hogben, T. Biskup, M. Ahmad, E. Schleicher, S. Weber, C. R. Timmel, and P. J. Hore, *Proc. Natl. Acad. Sci. USA* **109**, 4774 (2012).
- [43] I. K. Kominis, *Phys. Rev. E* **80**, 056115 (2009).
- [44] G. E. Katsoprinakis, A. T. Dellis, and I. K. Kominis, *New J. Phys.* **12**, 085016 (2010).
- [45] A. T. Dellis and I. K. Kominis, *Chem. Phys. Lett.* **543**, 170 (2012).
- [46] C. R. Timmel, U. Till, B. Brocklehurst, K. A. McLauchlan, and P. J. Hore, *Mol. Phys.* **95**, 71 (1998).
- [47] J. N. Bandyopadhyay, T. Paterek, and D. Kaszlikowski, *Phys. Rev. Lett.* **109**, 110502 (2012).
- [48] C. T. Rodgers, S. A. Norman, K. B. Henbest, C. R. Timmel, and P. J. Hore, *J. Am. Chem. Soc.* **129**, 6746 (2007).
- [49] R. Muheim, *Photobiology: The Science of Life and Light*, edited by Lars Olof Björn (Springer, New York, 2008), pp. 465–478.

- [50] S. Kais, in *Advances in Chemical Physics*, edited by D. A. Mazziotti (Wiley, New York, 2007), Vol. 134, pp. 493–535.
- [51] Z. Huang and S. Kais, *Phys. Rev. A* **73**, 022339 (2006).
- [52] Q. C. Shi and S. Kais, *Chem. Phys.* **309**, 127 (2005).
- [53] Z. Huang and S. Kais, *Chem. Phys. Lett.* **413**, 1 (2005).
- [54] G. Vidal and R. F. Werner, *Phys. Rev. A* **65**, 032314 (2002).
- [55] I. A. Solov'yov, D. Chandler, and K. Schulten, *Biophys. J.* **92**, 2711 (2007).
- [56] H. Mouritsen, G. Feenders, M. Liedvogel, and W. Kropp, *Curr. Biol.* **14**, 1946 (2004).
- [57] A. S. Kiryutin, O. B. Morozova, L. T. Kuhn, A. V. Yurkovskaya, and P. J. Hore, *J. Phys. Chem. B* **111**, 11221 (2007).